



Adsorption of textile dye from aqueous solution onto a low cost conch shells

I. El Ouahabi^{1,*}, R. Slimani¹, S. Benkaddour¹, H. Hiyane¹, N. Rhallabi²,
B. Cagnon³, M. El Haddad⁴, S. El Antri¹, S. Lazar^{1,*}

¹Laboratory of Biochemistry, Environment & Agroalimentary URAC 36, University of Hassan II-Casablanca, Mohammedia, Morocco

²Team of Microbiology, Hygiene & Bioactive Molecules, University of Hassan II-Casablanca, Mohammedia, Morocco

³Interfaces, Containment, Materials & Nanostructures, UMR 7374, CNRS-University of Orléans, La France.

⁴Team of Analytical Chemistry & Environment, University of Cadi Ayyad, Safi, Morocco

Received 04 Sep 2017,
Revised 09 Oct 2017,
Accepted 14 Oct 2017

Keywords

- ✓ Adsorption,
- ✓ Conch shells,
- ✓ Basic Yellow 28,
- ✓ Adsorption kinetics,
- ✓ Isotherm

Lazar_said@yahoo.fr /
imane.fstm@gmail.com ;
Phone: +212523314705;
Fax: +212523315353.

Abstract

The objective of this study was to investigate the adsorption of Basic Yellow 28 that is a cationic dye on conch shells. The factors affecting the adsorption process such as the initial concentration of the dye, pH of the solution, the adsorbent dosage and the time of contact were investigated in a batch-adsorption technique. The removal efficiency of Basic yellow 28 dye with an initial concentration of 25 mg/L was greater than 95% for 120 min contact time. The Freundlich adsorption isotherm provided adequate fit for the equilibrium adsorption data ($R^2 > 0.99$), while the pseudo second order rate equation described the kinetic adsorption data quite well ($R^2 > 0.99$). Kinetic studies showed that film diffusion and intra-particle diffusion were simultaneously operating during the adsorption process. A temperature uptake from 20°C to 50°C induced a decrease of adsorption for of Basic Yellow 28 and the process was found to be exothermic and spontaneous. It may be concluded that conch shells may be used as low-cost adsorbent for the removal of Basic Yellow 28 and it may also be effective in removing as well other harmful or undesirable species present in the wastewater.

1. Introduction

The effluents of textile, paper, food, plastic and cosmetic industries contain various organic dyes and pigments, the disposal of which causes environmental and water pollution [1-5]. Today, dyes play a critical role in textile, paint and pigment manufacturing industries, and at least 100,000 different dye types are commercially available currently [6,7]. To meet industrial demand, it is estimated that 1.6 million tons of dyes are produced annually, and 10-15% of this volume is discarded as wastewater [8,7]. Textile wastewater is an amalgam of pollutants but mainly it is characterized by high levels of Chemical Oxygen Demand (COD), Biological Oxygen Demand (BOD), dissolved solids and colors [9-11]. The dye-containing wastewater with high organic concentration and high chroma can cause severe environmental pollution and can have adverse impacts on human health if discharged without any treatment [12]. In recent decades, several physical, chemical and biological techniques have been reported to remove dyes from wastewater including like as biological treatment [13], chemical oxidation [14], ozone treatment [15], ion exchange [16], photocatalysis [17] and activated carbon adsorption [18]. Among the numerous techniques designed for dye removal, adsorption is one of the most effective, and it has been successfully employed-for-its simplicity, low-cost and easy availability of adsorbents [19-23]. Recently the researchers have focused their attentions to utilize low cost and efficient, locally available materials for the removal of dyes from water. In this regard, some low cost adsorbents such as montmorillonite [24,25], peanut husk [26], mussel shells [27], eggshells [28] and animal bone meal [29,30] have been tried successfully.

The aim of this present work is to valorize conch shells as a nonconventional, natural, low-cost adsorbent for removal of a reactive dye as Basic yellow 28 from aqueous solution by adsorption. Adsorption studies were carried out under various parameters such as pH, contact time, initial dye concentration and temperature. Also, isotherm and kinetic models were applied to the experimental data.

2. Material and Methods

2.1. The dye

The Basic Yellow 28 was selected in the present study as a representative cationic dye and abbreviated as BY 28, it was obtained from a local textile factory in Casablanca (Morocco) and used without further purification. It's particularly suitable for dyeing of paper, leather, and textile. The chemical structure and some properties of the dye are given respectively in Figure 1 and Table 1.

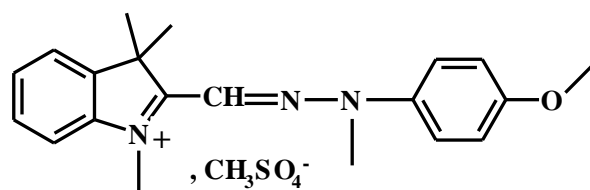


Figure 1: Chemical structure of Basic Yellow 28

Table 1: Some properties of BY 28 dye [31,32]

Color index	Basic Yellow 28
Commercial name	Maxilon Golden Yellow GL 200%
Shape	Powder 200%, particular 200%, liquid 200%
IUPAC name	2-[[[(4-methoxyphenyl)methylhydrazono]methyl]-1,3,3-trimethyl-3H-indolium methyl sulfate
CI number	48054
K values	3.0
F values	0.46
Solubility	90°C, 80 g/L 60°C, 60 g/L 30°C, 40 g/L
pH stability	3-10
Type	Cationic
Molecular Weight	433 g/mol
Azo group number	1
λ_{\max}	436 nm

2.2. Preparation of conch shells powder

The conch shells were collected from peage of Casablanca city in Morocco. They were repeatedly washed several times with tap water followed by distilled water and then were dried in oven at 100°C for 12 h. The dried shells conchs are crushed, powdered to small grains. Finally, the sieved material was treated with sodium hydroxide NaOH (2N) for 2 hours in a flask heated with reflux, then the sample was washed until neutralization and dried in the oven at 100°C for 24 h. The residue was finely chopped and ground into small particles of different sizes in the range of 75-100 mm, milled in an agate mortar, washed with distilled water, dried overnight at 105°C. The resulting material was stored in a glass bottle for further use without any pre-treatment and the resulting material was denominated conch shells treated (CST).

2.3. Adsorption studies

Batch equilibrium experiments were conducted by adding CST powder to a set of 250 mL conical flasks containing 100 mL of BY 28 solutions at a constant agitation rate of 250 rpm by varying the pH of solution from 3 to 11, the adsorbent dosage from 0.4 to 6 g/L, the contact time from 5 to 240 min, the initial dyes concentrations from 25 to 55 mg/L, the effects of ionic strength were studied by a wide range of NaCl from 2 to 10 mmol and the temperature from 20 to 50°C. The pH values were adjusted during the experiments by adding a few drops of dilute NaOH or HCl.

After adsorption, the reaction mixture was centrifuged to collect the supernatant solution at a rotational rate of 12000 rpm (Centrifugal type JA 10) for 15 min and it was used to measure the concentration of BY 28 by measuring absorbance at $\lambda_{\max}=436$ nm using UV-vis spectroscopy (BioMate 6, England). The point of zero charge (pHpzc) of CST was determined by salt addition method as described by Chun and Muhammad [33,34]. 100 mg of the sample was added to 98 mL of 0.01 M sodium chloride (NaCl) solution. The pH of the suspension was adjusted to 3.0-11.0 by adding HCl (1N) or NaOH (1N). The dispersions were shaken for 8 hours at ambient temperature, and the final pH of the solutions (pH_f) was determined. The pH_{pzc} of the sample

was calculated by plotting ΔpH (final pH - initial pH) versus pH_i . The value obtained at the intersection of the initial pH_i with the ΔpH gives the pH_{pzc} of the suspended solid.

The amount of adsorbate adsorbed at any time t , q_t (mg/g), was calculated using the following equation:

$$q_e = \frac{(C_o - C_t)}{W} V \quad (1)$$

where W is the mass of adsorbent expressed in g, V is the volume of the solution in L and C_o and C_t are the liquid-phase concentrations of BY 28 at initial and any time t respectively, expressed in mg/L. The dye removal percentage was calculated using the following equation:

$$\% \text{ of adsorption} = \frac{(C_o - C_e)}{C_o} * 100 \quad (2)$$

2.4. Adsorption kinetics

To investigate the adsorption mechanism of Basic yellow 28 onto the conch shells treated three kinetic models namely pseudo-first order, pseudo-second order and intraparticle diffusion were applied. These models are expressed by following equations [35,38]:

$$\text{Pseudo-first order} \quad \ln(q_e - q_t) = \ln(q_e) - k_1 t \quad (3)$$

$$\text{Pseudo-second order} \quad \frac{t}{q_t} = \frac{1}{k_2 q_e^2} + \frac{t}{q_e} \quad (4)$$

$$\text{Intra-particle diffusion} \quad q_t = k_{ID} \sqrt{t} + S \quad (5)$$

Where q_e and q_t (mg/g) are amount of adsorbate adsorbed at equilibrium and time t (min), respectively; k_1 (min^{-1}), k_2 (g/mg min) and K_{ID} ($\text{mg/g min}^{0.5}$) are the rate constants of pseudo-first order model, pseudo-second order model and the Intra-particle diffusion, respectively. S is a constant of intraparticle diffusion model which represents the thickness of boundary layer.

The applicability of the kinetic and isotherm model to describe the adsorption process was validated by the normalized standard deviation, Δq (%), which is defined as [39]:

$$\Delta q(\%) = 100 \sqrt{\frac{\sum [(q_{e,exp} - q_{e,cal}) / q_{e,exp}]^2}{N-1}} \quad (6)$$

where N is the number of data points, $q_{e,exp}$ and $q_{e,cal}$ (mg/g) are the experimental and calculated adsorption capacities, respectively. Lower value of Δq (%) indicates good fit between experimental and calculated data

2.5. Adsorption isotherms

The adsorption isotherm indicates how the molecules distribute between the liquid and solid phases when the adsorption process reaches equilibrium. It is important in describing how solutes interact with adsorbents, and is critical in optimizing the use of adsorbents [40]. Analysis of the isotherm data by fitting them to different isotherm models is an important step in finding the suitable model that can be used for design purposes [41].

Five common isotherm equations were tested in the present study: Langmuir [42], Freundlich [43], Temkin [44], Elovich [45] and Dubinin-Radushkevich [27]. The models used are shown in Table 2.

Table 2: Isotherm models tested in this study

Isotherm	Nonlinear form	Linear form	plot
Langmuir	$\frac{q_e}{q_m} = \frac{K_L C_e}{1 + K_L C_e}$	$\frac{C_e}{q_e} = \frac{1}{q_m K_L} + \frac{C_e}{q_m}$	$\frac{C_e}{q_e}$ vs. C_e
Freundlich	$q_e = K_F C_e^n$	$\log(q_e) = \log(K_F) + n \log(C_e)$	$\log(q_e)$ vs. $\log(C_e)$
Elovich	$\frac{q_e}{q_m} = K_E C_e \exp(-\frac{q_e}{q_m})$	$\ln \frac{q_e}{q_m} = \ln(K_E C_e) - \frac{q_e}{q_m}$	$\ln \frac{q_e}{q_m}$ vs. q_e
Temkin	$\frac{q_e}{q_m} = \frac{RT}{\Delta Q} \ln(K_T C_e)$	$q_e = B_T \ln K_T + B_T \ln C_e$ (with $B_T = \frac{q_m RT}{\Delta Q}$)	q_e vs. $\ln C_e$
Dubinin-Radushkevich	$q_e = q_m \exp(-\beta \varepsilon^2)$ (with $\varepsilon = RT \ln(1 + \frac{1}{q_e})$)	$\ln(q_e) = \ln(q_m) - \beta \varepsilon^2$	$\ln(q_e)$ vs. ε^2

2.6. Thermodynamic studies

The thermodynamic behavior of BY 28 adsorption on CST was demonstrated by evaluation of the changes in Gibbs free energy (ΔG°), enthalpy (ΔH°), and entropy (ΔS°) using following equations [27-30]:

$$\ln(k_d) = \frac{\Delta S}{R} - \frac{\Delta H}{RT} \quad (6)$$

$$\Delta G = -RT \ln(K_d) \quad (7)$$

where, K_d is equilibrium constant, R (J/mol K) represents the gas constant (8.314) and T (K) is the adsorption temperature.

3. Results and discussion

3.1. Characterization of CST adsorbent

The analysis of the chemical composition shows that CST is rich in oxygen (48.2%), which represents the main chemical species in the presence of other elements with small amounts, such as calcium (37.5%), carbon (11.9%), silicon (0.67%), sodium (0.61%), magnesium (0.31%), strontium (0.30%) and traces of other elements such as aluminum, iron, copper, sulfur, zinc, phosphorus and iodine. The X-ray diffraction of our adsorbent shown in Fig. 2. shows a main peak identified in the range $2\theta = 20-60$ are $2\theta = 26.28, 29.48^\circ, 33.19, 36.10, 37.95, 42.95, 45.92,$ and 48.95 . These correspond to those of the calcite and Aragonite as deduced by comparison with the data file ICDD reference number structure. 84-1998.

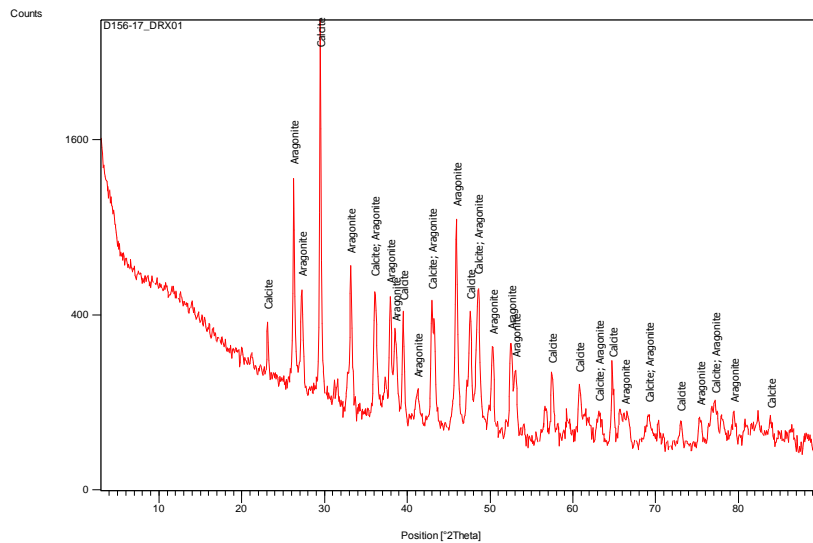


Figure 2: DRX of CST

FTIR analysis was performed in the range of $400-4000 \text{ cm}^{-1}$ with resolution 4 (20 scans) in order to explore the surface characteristics of the adsorbent. Figure 3 shows the FTIR spectrum of CST.

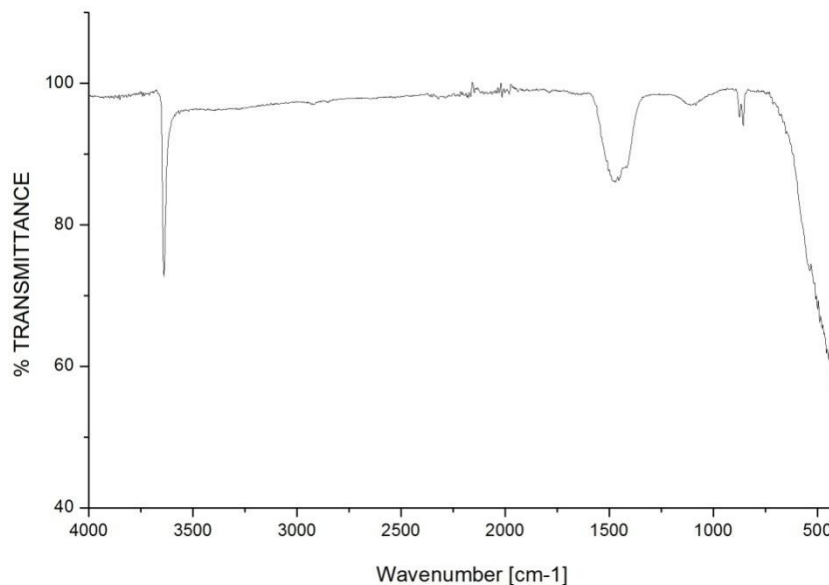


Figure 3: IRTF of CST

The peak positions showing major adsorption bands were observed at 3636, 1465, 855 and 420 cm^{-1} . The band at 3636 cm^{-1} is due to stretch vibration O-H, the band at 1465 may represent C=C aromatic stretch vibration, and the band at 855 cm^{-1} represents O-H stretch vibration.

The surface morphology of CST adsorbent observed by SEM depicted in Figure 4 indicates that the CST consists of tiny particles of various sizes.

The pH_{pzc} of the sample was calculated by plotting ΔpH (final pH - initial pH) versus pH_i . The value obtained at the intersection of the initial pH_i with the ΔpH in Figure 5 gives the pH_{pzc} of the suspended solid. From Figure 5 the pH_{pzc} of CST is found around 8.9.

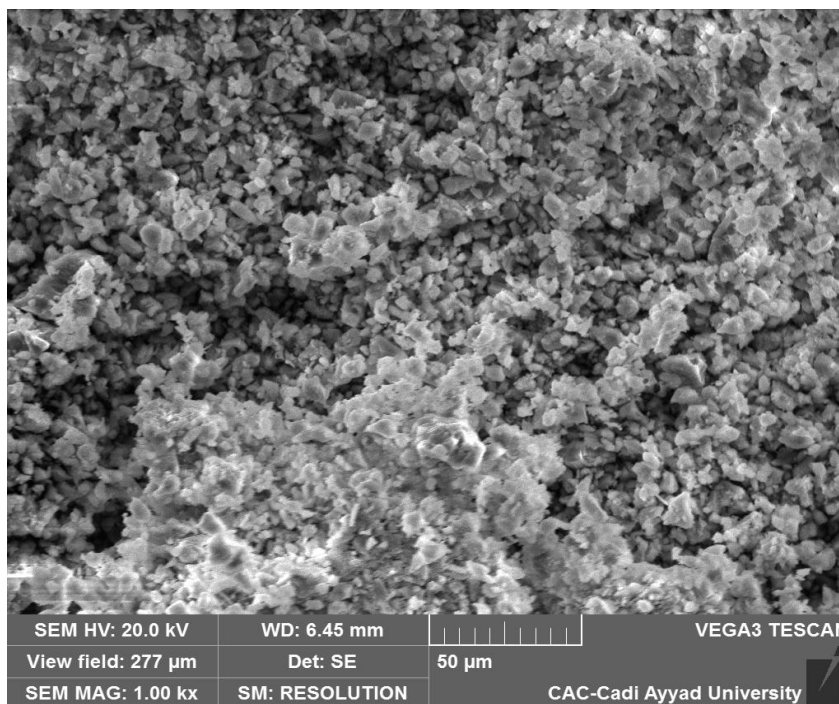


Figure 4: SEM of CST

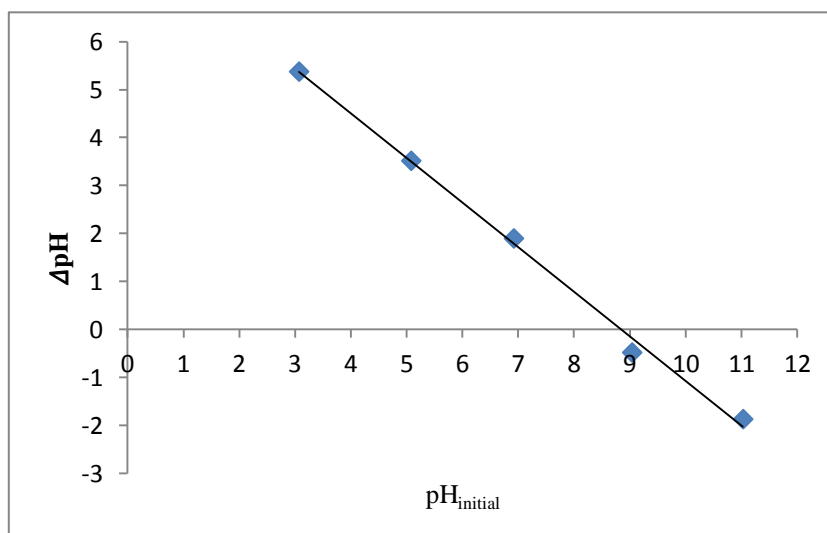


Figure 5: Determination of pH_{pzc} of the CST

3.2. Influence of the adsorbent dose on the adsorption of BY 28

It is well recognized that the amount of adsorbent is an important parameter that affects adsorption capacity. In order to observe the minimum possible amount which shows maximum adsorption. The effect of dose of CST onto BY 28 was studied by changing the quantity of adsorbent from 0.4 - 6 g/L in 100 mL of dye solution and keeping unchangeable the initial dye concentration at 25 mg/L, ambient temperature and initial pH of the dye solution. It was seen from Figure 6 that removal of dye increased from 91.37 to 98.07% , this can be attributed by increased surface area and the adsorption sites, as already reported [46,47].

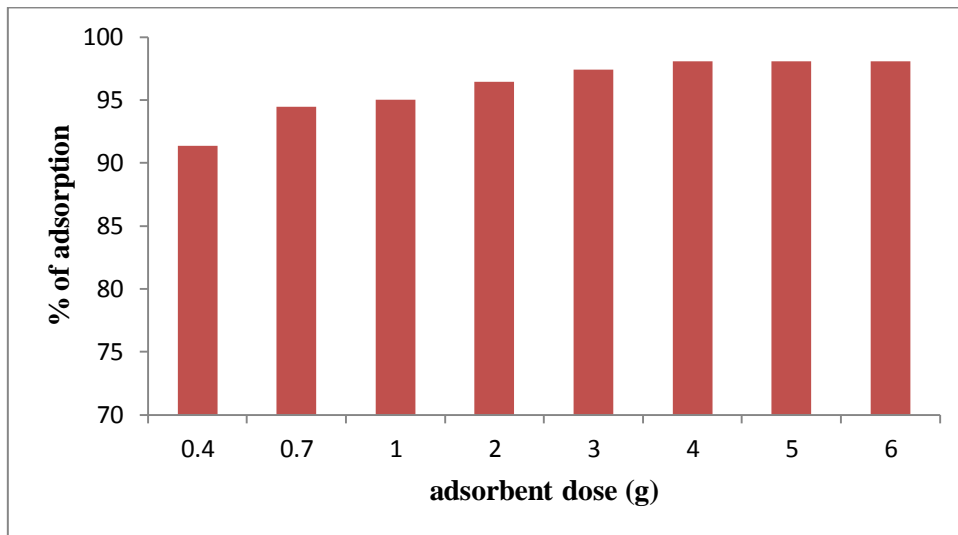


Figure 6: Effect of adsorbent dose on the adsorption of BY 28 on CST

3.3. Influence of initial dye concentration and time on the adsorption of BY 28

The contact time is inevitably a fundamental parameter in all transfer phenomena such as adsorption. The effect of the initial concentration of BY 28 dyes on the removal efficiency of the CST was studied at different initial concentrations of dye (25, 30, 35, 40, 45, 50 and 55 mg/L), keeping other parameters constant. As can be seen in Figure 7, the removal efficiency of BY 28 onto CST by adsorption is rapid initially and then slows down gradually until it attains equilibrium. The increase in the adsorption capacity in the first 45 min was very rapid. This might be due to the diffusion of dye molecules into the surface pores of the CST granules, but with the progresses of time, the active sites get occupied due to competitive adsorption of sorbate molecules. Equilibrium is deduced to have been attained within 120 min for all of the studied concentrations. Figure 7 shows the adsorption capacity increased with an increase in the dye concentration. We propose that an increase in the initial dye concentration leads to an increase in the mass gradient between the solution and the adsorbent and thus acts as a driving force for the transfer of dye molecules from solution to the surface of CST. The increase in the proportional dye adsorption is attributed to an equilibrium shift during the CST adsorption process [48].

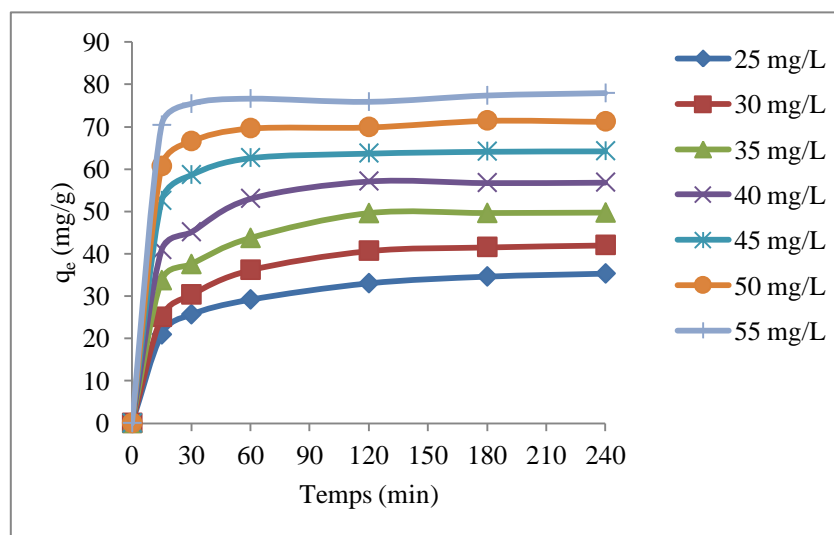


Figure 7: Effect of contact time and initial dye concentration on adsorption of BY 28 dye onto CST

3.4. Influence of pH on the adsorption of BY 28 onto CST

The initial pH of the dye solution is an important parameter, which controls the adsorption process particularly the adsorption capacity. pH of the solution may change: (1) the surface charge of the adsorbent, (2) the degree of ionization of the adsorbate molecule and (3) extent of dissociation of functional groups on the active sites of the adsorbent [49]. The variation in the adsorption of the dye was studied in the pH range of 3-11, and the results are shown in Figure 8. It is observed that uptake increases from 12.58 to 34.08 mg/g for an increase in pH from 3 to 11.

The pH_{pzc} of CST have shown that CST exhibits a negative charge at pH>8.9 and yields a positive charge at pH<8.9. The BY 28 dye is a cationic compound. Therefore, the higher uptake of BY 28 on CST at high pH may result to the neutralization of the negative charge at the surface of adsorbent. A slight decrease in the amount dye adsorbed with decreasing pH may be due to the repulsion between species with the same charge, i.e., the dye molecule and the surface of CST.

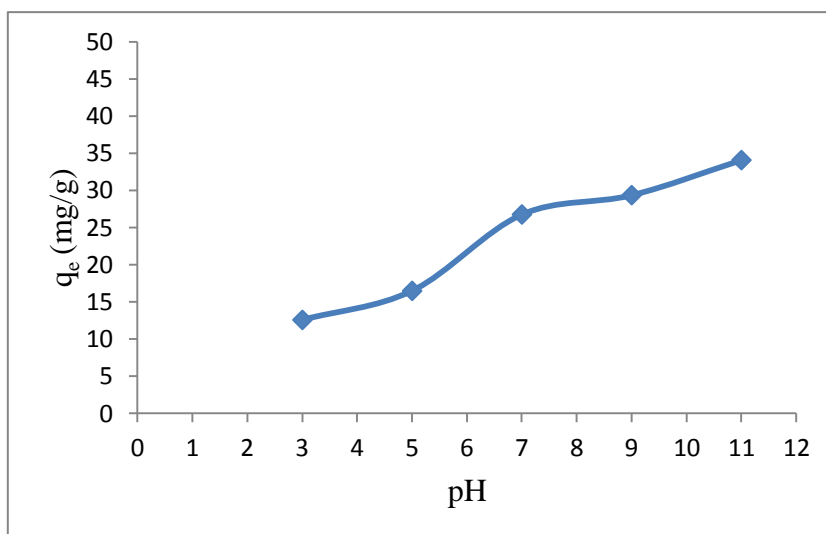


Figure 8: Effect of pH on BY 28 adsorption onto CST

3.5. Influence of ionic strength on the adsorption of BY 28 onto CST

The presence of different electrolytes in the solution plays an important role on dye adsorption. It is known that salts can either accelerate or retard the dye adsorption process. The salt may affect the adsorption either by screening the coulomb potential between the adsorbing molecule and the charged adsorbent, or by adsorbing preferentially on oppositely charged sites of the adsorbent [50,51].

To study the effect of ionic strength, the same type of adsorption experiments as discussed above were carried out in the presence of NaCl (2, 4, 8, 10 mmol). As can be seen in Figure 9, increasing the ionic strength of the solution causes a slight decrease in the adsorption of BY 28 onto the CST surface, which can be explained by the reduction of the electrostatic interaction between CST and dye.

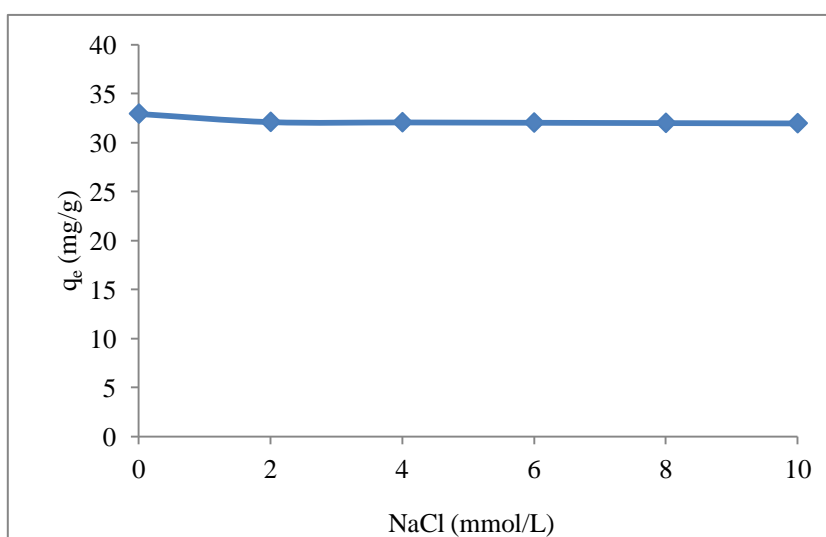


Figure 9: Effect of ionic strength on BY 28 adsorption

3.6. Influence of temperature on the adsorption of BY 28 onto CST

The effect of the solution temperature on BY 28 adsorption onto CST was investigated at various temperatures, 20°C, 30°C, 40°C, and 50°C and the results were shown in Figure 10. As shown in Figure 10, where increasing the temperature from 20°C to 50°C the amount of dye adsorbed decreases from 32.26 to 24.44 mg/g. It was due to the fact that the adsorptive forces between dye molecules and the active sites on the CST

became weak by increasing the temperature so that dye removal was decreased [52,53]. So, it can be concluded that the adsorption of BY 28 on the surface of CST is the exothermic process.

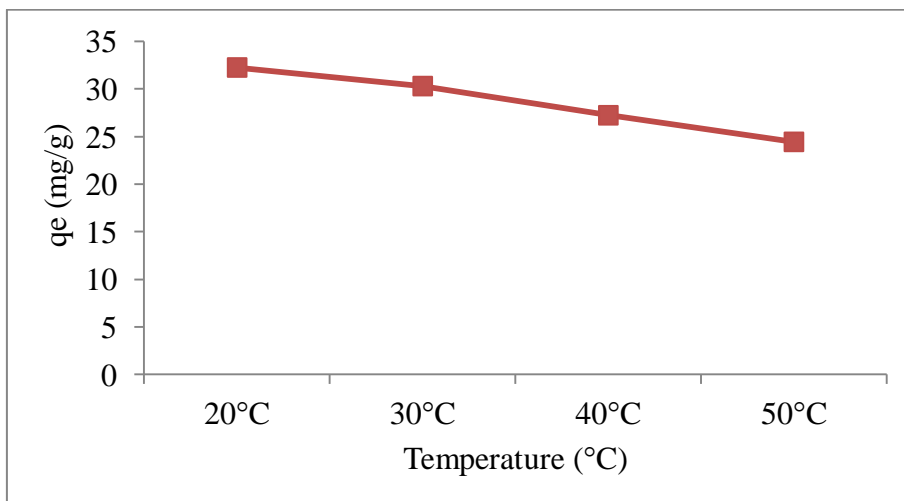


Figure 10: Effect of temperature on BY 28 adsorption

3.7. Adsorption Kinetics

Pseudo-first order, pseudo-second order and the intraparticle diffusion model were used to test dynamical experimental data. The kinetic models plots for adsorption of BY 28 on CST at different temperatures are shown in Figures 11 and 12, respectively. Calculated values of rate constants at different temperatures are shown in Table 3.

From Table 3, the R^2 values for pseudo-first order kinetic models are relatively good, and the values of normalized standard deviation are also high which is due to the calculated q_e values are too low compared with experimental q_e values. Also, the estimated values of q_e predicted by this model are not close to the experimental values, which show that this model is not appropriate to describe the investigated adsorption process. The correlation coefficients for the second order kinetic model were close to 1, and the lower normalized standard deviation values confirm that this one describes correctly the adsorption kinetics.

The plot of Intra-particle diffusion kinetic models for adsorption of BY 28 onto CST is shown in Figure 13. Based on this figure, it may be seen that the intra-particle diffusion of BY 28 within the CST occurred in tow separate regions the initial part is attributed to the bulk diffusion while the final part to the intraparticle diffusion [54-56]. The intraparticle diffusion constants and regression coefficients (k_{ID} and R^2) are given in Table 3.

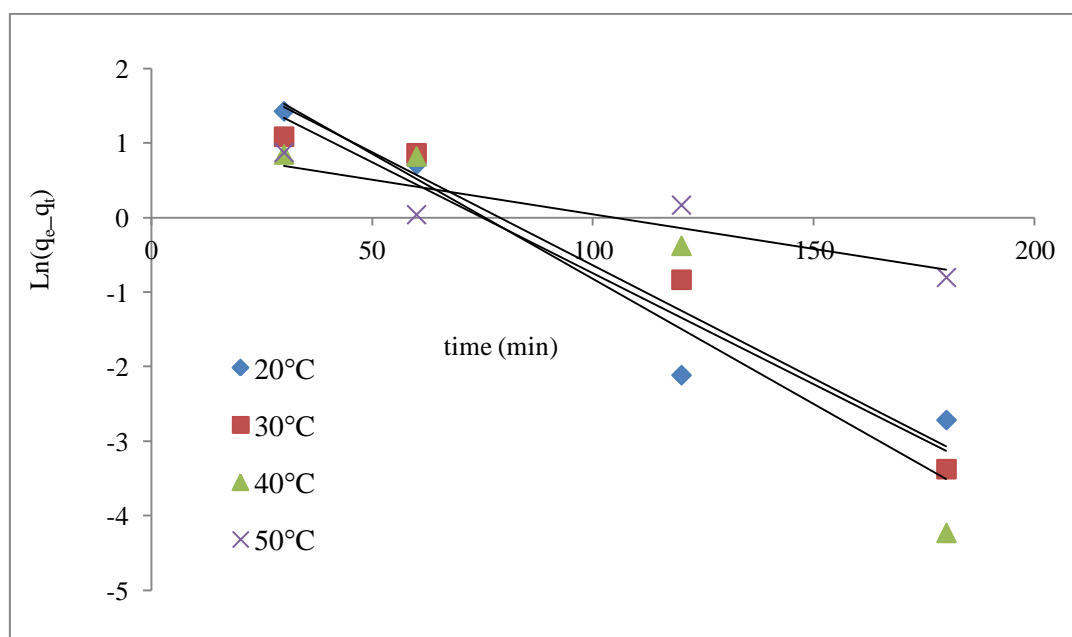


Figure 11: Pseudo-first order adsorption kinetics of BY 28 on CST at different temperatures

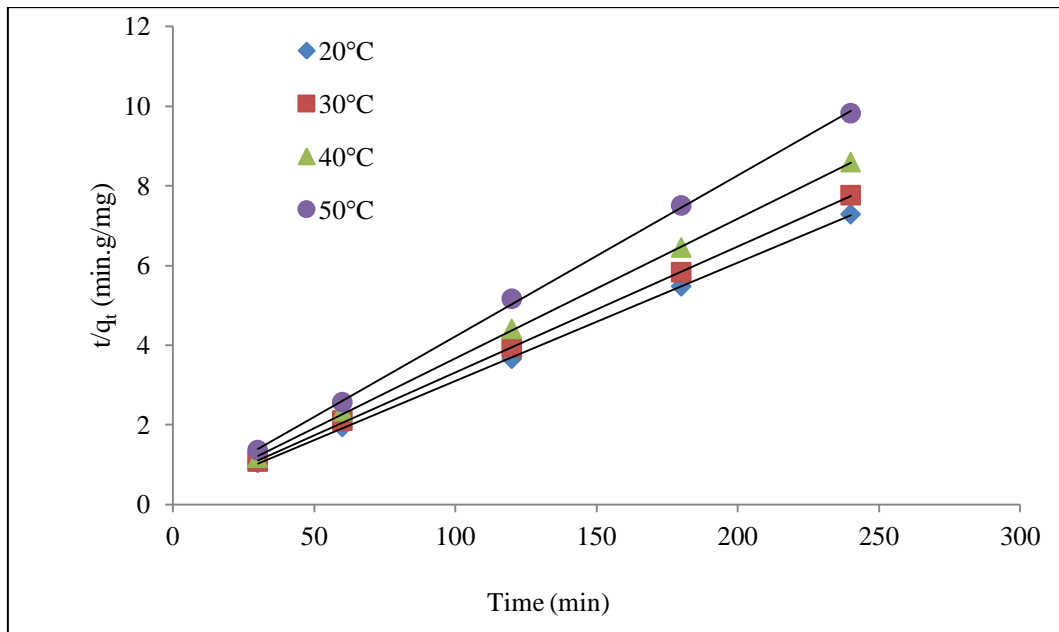


Figure 12: Pseudo-second order adsorption kinetics of BY 28 on CST at different temperatures

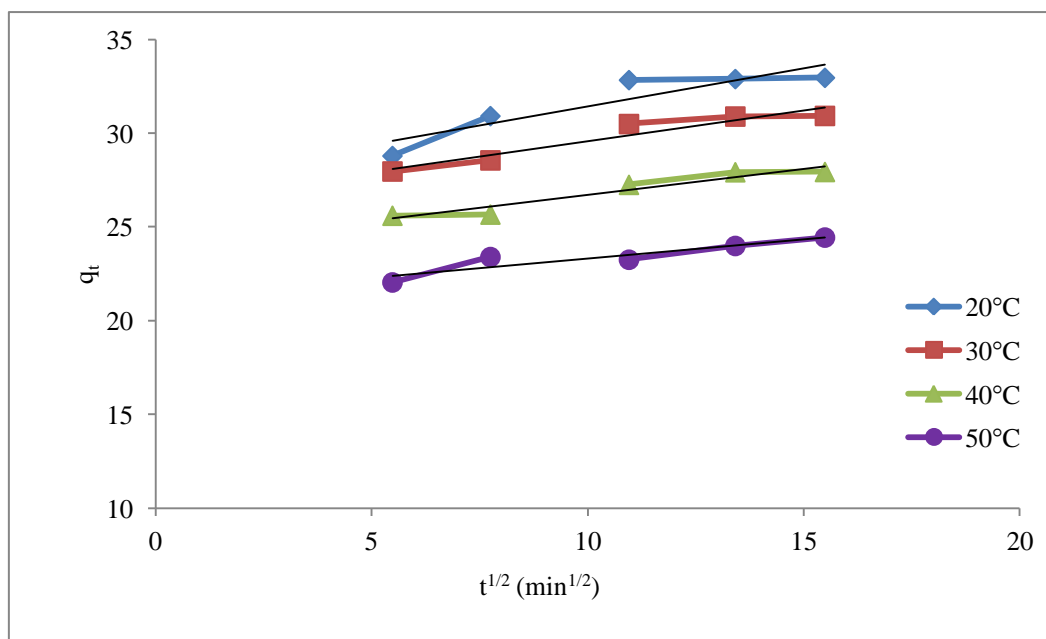


Figure 13: Intra-particle diffusion model of BY 28 on CST at different temperatures

Table 3: Calculations constants kinetics model for adsorption of BY 28 on CST

T (°C)	Pseudo-first order model				Pseudo-second order model				Intra-particle diffusion model			
	$q_{e,exp}$ (mg/g)	k_1 (min ⁻¹)	$q_{e,cal}$ (mg/mg)	R^2	Δq (%)	k_2 (g/mg.min)	$q_{e,cal}$ (mg/mg)	R^2	Δq (%)	K_{ID} (mg/g.min ^{1/2})	S (mg/g)	R^2
20	32.96	0.029	9.27	0.930	71.87	0.0060	34.48	0.994	4.62	0.407	27.35	0.824
30	30.93	0.030	10.96	0.956	64.57	0.0063	32.26	0.993	4.291	0.328	26.28	0.910
40	27.94	0.033	12.63	0.865	54.80	0.0070	28.57	0.992	2.26	0.274	23.96	0.920
50	24.44	0.035	14.01	0.802	42.67	0.0086	25.00	0.996	2.27	0.205	21.25	0.854

3.8. Isotherms

The equilibrium adsorption data of BY 28 onto CST adsorbent was analyzed using Langmuir, Freundlich, Temkin, Elovich and Dubinin-Radushkevich models. The isotherm constants of each model were calculated and presented in Table 4.

The results showed that the equilibrium data of adsorption BY 28 onto CST were well fitted by the Freundlich isotherm model with an R^2 value 0.993 as compared to the other isotherm equations. The value of n , which is significantly lower than unity, indicated that the BY 28 dye is favourably adsorbed by CST. The Freundlich isotherm theory indicates multilayer adsorption with interaction between adsorbed molecules and also the heterogeneous distribution of active sites on the material, since the model presupposes that the surface is heterogeneous [43].

Table 4: The isotherms constants related to the adsorption of BY 28 dye onto CST

Isotherm model	Parameters				
Langmuir	$K_L = 0.0971 \text{ L/mg}$	$q_m = 333.333 \text{ mg/g}$	$R_L = 0.292$		$R^2 = 0.932$
Freundlich	$K_F = 29.195 \text{ mg}^{1-n} \cdot \text{L}^n/\text{g}$		$n = 0.386$		$R^2 = 0.993$
Elovich	$K_E = 0.130 \text{ L/mg}$		$q_m = 250 \text{ mg/g}$		$R^2 = 0.888$
Temkin	$K_T = 1.702 \text{ L/mg}$	$\Delta Q = 19.292 \text{ KJ/mol}$		$B_T = 42.83$	$R^2 = 0.986$
D-R	$q_m = 87.095 \text{ mg/g}$	$\beta = 5 \cdot 10^{-7}$		$E = 10 \text{ KJ/mol}$	$R^2 = 0.965$

3.7. Thermodynamic parameters

Based on fundamental thermodynamic concept, the ΔG° , ΔH° and ΔS° values for the adsorption of BY28 onto CST were calculated from the slope and intercept of Van't Hoff plots of $\ln K_d$ versus $1/T$ (Figure 14) and presented in Table 5.

The negative values of ΔH° (-38.311 kJ/mol) in the range of 20 - 50°C show that the adsorption of BY 28 onto CST is exothermic in nature. The negative ΔG° values -6.315, -5.243, -3.969 and -3.038 kJ/mol at 20, 30, 40 and 50°C respectively confirm that adsorption of BY 28 onto CST is spontaneous, The negative values of ΔS° (-111.16 J/mol.K) suggested that the decrease randomness at the solid-solution interface during the adsorption of the dye on CST.

Table 5: Thermodynamic parameters for adsorption of BY 28 on CST

T (K)	ΔG° (kJ/mol)	ΔH° (kJ/mol)	ΔS° (kJ/mol.K)
293	-6.315		
303	-5.243		
313	-3.969	-38.310	-0.111
323	-3.038		

3.8. Comparison of adsorbents

A comparative evaluation of the adsorbent capacities of various types of adsorbents for the adsorption of basic dyes is listed in Table 6. The adsorption capacities of the adsorbents used in this study were not among the highest available but a relatively high uptake capacity of the dye could be obtained which makes the adsorbents suitable for colors removal in textile industry

Table 6: Maximum adsorption capacity of various basic dyes by some adsorbents

Adsorbent	Adsorbate	q_m (mg/g)	References
calcined mussel shells	BY 28	47.3	[27]
Calcined eggshells	BY 28	23.31	[28]
calcined bones	Direct Red 75, Direct Red 80	65.78, 63.78	[29]
Clinoptililite	BY 28	59	[57]
Green alga	BY 28	27	[6]
Bagasse pith	Basic Red 22, Basic Blue 69	18, 16	[58]
CST	BY 28	78.22	This study

Conclusion

This study investigated the equilibrium and the dynamics of the adsorption of basic dyes on conch shells treated. The adsorption of BY 28 was found to be dependent on concentration, temperature, pH, contact time and adsorbent amount. It was found that the adsorption of BY 28 onto CCT is favourable at basic pH and high temperature. Adsorption kinetics followed pseudo-second order kinetics model. The experimental data were examined using five adsorption models and it was found that the Freundlich model represented the best fit of experimental data. That indicates the multilayer adsorption and the heterogeneous distribution of active sites on the material. The ΔG° values for the dyes were negative -6.315, -5.234, -3,969 and -3,038 kJ/mol were reported

at 20°C, 30°C, 40°C, and 50°C, respectively, therefore, the adsorption was spontaneous and favourable at high temperature, the negative value of ΔS° (-111.16 J/mole.K) suggests a decreased randomness at the solid/solution interface. Based on the results, it was concluded that CST had a significant potential for removing basic dye from wastewater using the adsorption method.

Acknowledgements-The authors thank the CNRST for its financial support of PPR2/2016/21.

References

1. A.S. Alzaydien, *Am. J. Environ. Sci.* 5 (2009) 197-208.
2. A.M. Donia, A.A. Atia, W.A. Al-Amrani, A.M. Ei-Nahas, *J. Hazard. Mater.* 161 (2008) 1544-1550.
3. A. Hou, B. Chen, J. Dai, K. Zhang, *J. Clean. Prod.* 18 (2010) 1009-1014.
4. M. Ilayarajaa, N.P. Krishnanb, R. Sayee Kannana, *J. Environ. Sci. Toxicol. Food Technol.* 5 (2013) 79-89.
5. D. Sasmal, J. Maity, H. Kolya, T. Tripathy, *J. Water Process Eng.* 18 (2017) 7-19.
6. V.K. Gupta, Suhas, *J. Environ. Manage* 90 (2009) 2313-2342.
7. K.B. Tan, M.T. Vakili, B.A. Horri, P.E. Poh, A. . Abdullah, B. Salamatinia, *Sep. Purif. Technol.* 150 (2015) 229-242
8. K. Hunger, *Industrial Dyes - Chemistry, Properties, Application*, Wiley, 2003.
9. D.J. Naik, H.H. Desai, T.N Desai, *India. J. Environ. Res. Dev.* 7 (2013) 1602-1605.
10. A.E. Ghaly, R. Ananthashankar, M. Alhattab, V.V. Ramakrishnan, *J. Chem. Eng. Process. Technol.* 5 (2014) 1-18.
11. A. Wasti, M.A. Awan, *J. Assoc. Arab. Univ. Basic. Appl. Sci.* 20 (2016) 26-31.
12. Y. Pan, Y. Wang, A. Zhou, A. Wang, Z. Wu, L. Lv, X. Li, K. Zhang, T. Zhu, *Chem. Eng. J.* 326 (2017) 454-461.
13. M. Kornaros, G. Lyberatos, *J. Hazard. Mater.* 136 (2006) 95-102.
14. K. Dutta, S. Mukhopadhyay, S. Bhattacharjee, B. Chaudhuri, *J. Hazard. Mater.* 84 (2001) 57-71.
15. H. Selcuk, *Dyes Pigm.* 64 (2005) 217-222.
16. C.H. Liu, J.S. Wu, H.C. Chiu, S.Y. Suen, K.H. Chu, *Water. Res.* 41 (2007) 1491-1500.
17. M. Muruganandham, M. Swaminathan, *J. Hazard. Mater.* 135 (2006) 78-86.
18. I.A.W. Tan, A.L. Ahmad, B.H. Hameed, *J. Hazard. Mater.* 154 (2008) 337-346.
19. K. Santhy, P. Selvapathy, *Bioresour. Technol.* 97 (2006) 1329-1336.
20. H. Zhu, R. Jiang, Y.Q. Fu, J.H. Jiang, L. Xiao, G. M. Zeng, *Appl. Surf. Sci.* 258 (2011) 1337-1344.
21. M. Arshadi, F.S. Vahid, J. Salvacion, M. Soleymanzadeh, *Appl. Surf. Sci.* 280 (2013) 726-736.
22. SC. Ming, SC. Guo, *Chemosphere*, 62 (2006) 731-40
23. C. Djilani, R. Zaghoudi, F. Djazi, B. Bouchekima, A. Lallam, A. Modarressi, M. Rogalski, *J. Taiwan Inst. Chem. Eng.* (2015) 1-10.
24. B. Makhoukhi, M.A. Didi, H. Moulessehou, A. Azzouz, D. Villemin, *Appl. Clay. Sci.* 50 (2010) 354-361.
25. B. Makhoukhi, M.A. Didi, H. Moulessehou, A. Azzouz, *Mediterr. J. Chem.* 1 (2011) 44-55.
26. S. Sadaf, H.N. Bhatti, *Clean Technol. Environ. Policy* 16 (2014) 527-544.
27. I. El Ouahabi, R. Slimani, I. Hachoumi, F. Anouar, N. Taoufik, A. Elmchouari, S. Lazar, *Mediterr. J. Chem.* 4 (2015) 261-270.
28. R. Slimani, I. El Ouahabi, F. Abidi, M. El Haddad, S. El Antri, S. Lazar, *J. Taiwan. Inst. Chem. Eng.* 45 (2014) 1578-1587.
29. M. El Haddad, R. Slimani, R. Mamouni, S. El Antri, S. Lazar, *J. Assoc. Arab. Univ. Basic. Appl. Sci.* 14 (2013) 51-59.
30. R. Slimani, A. Anouzla, Y. Abrouki, Y. Ramli, S. El Antri, R. Mamouni, S. Lazar, M. El Haddad, *J. Mater. Environ. Sci.* 2 (2011) 77-87.
31. F. Gimbert, N. Morin-Crini, F. Renault, P.M. Badot, G. Crini, *J. Hazard. Mater.* 157 (2008) 34-46.
32. A. Kapoor, R. T. Yang, *Gas Sep Purif.* 3 (1989) 187-192.
33. H. Chun, W. Yizhong, T. Hongxiao, *Chemosphere* 41 (2000) 1205-1209.
34. S. Muhammad, S.T. Hussain, M. Waseem, A. Naeem, J. Hussain, M. Tariq Jan, *Iran. J. Sci. Technology A*, 4 (2012) 481-486.
35. S. Langergen, B.K. Svenska, *Eteruskapsakad Handl.* 24 (1898) 1-39.
36. Y.S. Ho, G. Mckay, *Process Biochem.* 34 (1999) 451-465.
37. G.E. Boyd, A. W. Adamson, L.S. Myers, *J. Am. Chem. Soc.* 69 (1947) 2836-2848.
38. F. Marrakchi, J.A. Muthanna, W.A. Khanday, M. Asif, B.H. Hameed, *J. Taiwan Inst. Chem. Eng.* (2016) 1-8.
39. S. Figaro, J.P. Avril, F. Brouers, A. Ouensanga, S. Gaspard, *J. Hazard. Mater* 161 (2009) 649-656
40. I.A. Tan, A.L. Ahmad, B.H. Hameed, *J. Hazard. Mater.* 154 (2008) 337- 346

41. H. Demiral, İ. Demiral, B. Karabacakoğlu, F. Tımsek, *J. Int. Environ. Appl. Sci.* 3 (2008) 381-389.
42. I. Langmuir, *J. Am. Chem. Soc.* 40 (1918) 1361-1403.
43. H.M.F. Freundlich, *J. Phys. Chem.* 57 (1906) 385-471.
44. M.I. Temkin, V. Pyzhev, *J. Phy. Chem USSR* 12 (1940) 327-356.
45. M. M. Dubinin, *Chem. Rev.* 60 (1960) 235-266.
46. R. Liu, B. Zhang, D. Mei, H. Zhang, J. Liu, *Desalination* 268 (2010) 111-116.
47. S. Lairini, K. El Mahtal, Y. Miyah, K. Tanji, S. Guissi, S. Boumchita, F. Zerrouq, *J. Mater. Environ. Sci.* 8 (2017) 3252-3261.
48. Y. Cheng, Q. Feng, X. Ren, M. Yin, Y. Zhou, Z. Xue, *Colloids. Surf. A. Physicochem. Eng. Asp.* 485 (2015) 125-135.
49. B.K. Nandi, A. Goswami, M.K. Purkait, *J. Hazard. Mater.* 161 (2009) 387-395.
50. G. Crini, P. M. Badot, *Prog. Polym. Sci.* 33 (2008) 399-447.
51. H. Momenzadeh, A.R. Tehrani-Baghab, A. Khosravi, K. Gharanjig, K. Holmberg, *Desalination.* 271 (2011) 225-230.
52. M.T. Yagub, T.K. Sen, S. Afroze, H.M. Ang, *Adv. Colloid. Interface. Sci.* 209 (2014) 172-184.
53. A.E. Ofomaja, Y. S. Ho, *Dyes. Pigm.* 74 (2007) 60-66.
54. S.J. Allen, G. McKay, K.Y.H. Khader, *Environ. Pollut.* 56 (1989) 39-50.
55. B. Koumanova, P. Peeva, S. J. Allen, *J. Chem. Technol. Biotechnol.* 78 (2003) 582-587.
56. M.F.F. Sze, G. McKay, *Environ. Pollut.* 158 (2010) 1669-1674.
57. J. Yener, T. Kopac, G. Dogu, T. Dogu, *J. Colloid Interf. Sci.* 294 (2006) 255-264.
58. V. Meshko, L. Markovska, M. Mincheva, A.E. Rodrigues, *Water Res.* 35 (2001) 3357-3366.

(2018) ; <http://www.jmaterenvironsci.com>